

ARMY RESEARCH LABORATORY



Mechanisms of Superplastic Deformation of Nanocrystalline Silicon Carbide Ceramics

by Yutaka Shinoda

ARL-CR-702

August 2012

NOTICES

Disclaimers

The findings in this report are not to be construed as an official Department of the Army position unless so designated by other authorized documents.

Citation of manufacturer's or trade names does not constitute an official endorsement or approval of the use thereof.

Destroy this report when it is no longer needed. Do not return it to the originator.

Army Research Laboratory

Aberdeen Proving Ground, MD 21005-5066

ARL-CR-702

August 2012

Mechanisms of Superplastic Deformation of Nanocrystalline Silicon Carbide Ceramics

Yutaka Shinoda
Tokyo Institute of Technology

REPORT DOCUMENTATION PAGE			Form Approved OMB No. 0704-0188		
Public reporting burden for this collection of information is estimated to average 1 hour per response, including the time for reviewing instructions, searching existing data sources, gathering and maintaining the data needed, and completing and reviewing the collection information. Send comments regarding this burden estimate or any other aspect of this collection of information, including suggestions for reducing the burden, to Department of Defense, Washington Headquarters Services, Directorate for Information Operations and Reports (0704-0188), 1215 Jefferson Davis Highway, Suite 1204, Arlington, VA 22202-4302. Respondents should be aware that notwithstanding any other provision of law, no person shall be subject to any penalty for failing to comply with a collection of information if it does not display a currently valid OMB control number. PLEASE DO NOT RETURN YOUR FORM TO THE ABOVE ADDRESS.					
1. REPORT DATE (DD-MM-YYYY) August 2012		2. REPORT TYPE Final		3. DATES COVERED (From - To) October 2008–September 2010	
4. TITLE AND SUBTITLE Mechanisms of Superplastic Deformation of Nanocrystalline Silicon Carbide Ceramics			5a. CONTRACT NUMBER FA 5209-09-0272		
			5b. GRANT NUMBER		
			5c. PROGRAM ELEMENT NUMBER		
6. AUTHOR(S) Yutaka Shinoda			5d. PROJECT NUMBER AH80		
			5e. TASK NUMBER		
			5f. WORK UNIT NUMBER		
7. PERFORMING ORGANIZATION NAME(S) AND ADDRESS(ES) Tokyo Institute of Technology 4259-R3-23 Nagatsuta-Cho Midori-Ku Yokohama 226-8503, Japan			8. PERFORMING ORGANIZATION REPORT NUMBER		
9. SPONSORING/MONITORING AGENCY NAME(S) AND ADDRESS(ES) U.S. Army Research Laboratory ATTN: RDRL-WM Aberdeen Proving Ground, MD 21005-5066			10. SPONSOR/MONITOR'S ACRONYM(S)		
			11. SPONSOR/MONITOR'S REPORT NUMBER(S) ARL-CR-702		
12. DISTRIBUTION/AVAILABILITY STATEMENT Approved for public release; distribution is unlimited.					
13. SUPPLEMENTARY NOTES					
14. ABSTRACT This project was undertaken to obtain preliminary data on the effect of nanograin size SiC materials on its properties. Using starting SiC powders with an average particle size of about 30 nm and small amounts of carbon and oxygen impurities, several processing techniques were used to fabricate bulk samples. These included the following: standard hot isostatic pressing (HIP), spark plasma sintering, ultra-high pressure HIP, and a multianvil pressure apparatus. The ultra-high pressure HIP technique achieved a final average grain size less than 100 nm and a relative percent of theoretical density of 96.8%; the hardness of this material was 22.7 GPa. A theoretical analysis of the effect of grain size on critical resolved shear stress to nucleate dislocations suggested a critical grain size of about 400 nm, below where it was easier to move partial dislocations. However, above this size, it was easier to move perfect dislocations. In addition, using more conventional hot-pressing techniques, the effect of different silicon and carbon contents was also investigated. It was found that increases in the free carbon and silicon content decreased the resulting grain size and influenced their strain rate sensitivity and flow stress.					
15. SUBJECT TERMS silicon carbide, nanostructure, sintering, hot isostatic pressing, hardness					
16. SECURITY CLASSIFICATION OF:			17. LIMITATION OF ABSTRACT	18. NUMBER OF PAGES	19a. NAME OF RESPONSIBLE PERSON James W. McCauley
a. REPORT Unclassified	b. ABSTRACT Unclassified	c. THIS PAGE Unclassified			UU

Contents

List of Figures	iv
List of Tables	v
Foreword	vi
1. Objective	1
2. Results	1
2.1 Fabrication of Nanocrystalline SiC Ceramics	1
2.2 The Effect of the Grain Size on the Deformation at Elevated Temperature	4
2.3 Participation and Morphology of Dislocation Activity in Deformation of Nano-SiC Ceramics.....	5
2.4 The Effect of Carbon Content on the Deformation at Elevated Temperature.....	7
Distribution List	10

List of Figures

Figure 1. Ultra-high pressure HIP; 1600 °C, 980 MPa.....	2
Figure 2. Multianvil high-pressure apparatus; 1200 °C, 3 GPa.	2
Figure 3. Standard HIP; 2000 °C, 200 MPa.....	3
Figure 4. Sinter forging by SPS; 1800 °C, 500 MPa.	3
Figure 5. Relationship between stress and strain rate of SiC with different grain sizes.....	4
Figure 6. Relationship between grain size and shear stress required for nucleation of dislocation.	5
Figure 7. TEM image before deformation.	6
Figure 8. TEM image of deformed SiC (1900 °C, $1 \times 10^{-4} \text{ s}^{-1}$, $\epsilon = 0.65$).	6
Figure 9. TEM image of annealed SiC (2100 °C, 1 h) after deformation.	7
Figure 10. SEM micrographs of hot-pressed SiC.....	8
Figure 11. Relationship between the amount of excess carbon and silicon and grain size.	9
Figure 12. Relationship between stress and strain rate.....	9

List of Tables

Table 1. Characteristics of sintered SiC by various sintering methods.....	1
Table 2. Hot-pressed SiC characteristics.	8

Foreword

This project has been co-funded by the U.S. Army International Technology Center - Pacific and the U.S. Army Research Laboratory (ARL) under the direction of Drs. J. W. McCauley and J. P. Singh of ARL.

1. Objective

The aim of the present study is to clarify the effect of the grain size and free-carbon content on the superplastic deformation in order to invent the high-performance nano-silicon carbide (SiC) ceramics and reveal the participation and morphology of dislocation activity in superplastic deformation of nano-SiC ceramics.

2. Results

2.1 Fabrication of Nanocrystalline SiC Ceramics

Nanocrystalline β -SiC powder with a mean particle size of 30 nm (Sumitomo-Osaka Cement Co., Tokyo, Japan, T-1 grade) was sintered without a sintering additive using several methods. The powder contained 3.7 weight-percent free carbon and 0.6 weight-percent impurity oxygen, and the amount of other metallic impurities was less than 1 ppm. Table 1 shows the characteristics of SiC sintered by various sintering methods. Figures 1–4 show the microstructure of the sintered SiC. The grain size decreased with decreasing sintering temperature. The grain size of the sintered body using multianvil apparatus was smallest; however, its hardness was extremely low in spite of relatively high density. The perfect bonding of SiC particles required a higher temperature than 1200 °C. The sintered body via the ultra-high pressure hot isostatic pressure (HIP) exhibited the highest density and highest hardness and fine grain size of less than 100 nm. The ultra-high pressure HIP was effective for fabricating high-quality nanocrystalline SiC ceramics.

Table 1. Characteristics of sintered SiC by various sintering methods.

Sintering Method	Sintering Conditions		Relative Density (%)	Hv (1 kgf) (kgf/mm ²)
	Temperature (C°)	Pressure (MPa)		
Standard HIP	2000	200	93.8	2000
Sinter forging by SPS	1800	500	93.5	2080
Ultra-high pressure HIP	1600	980	96.8	2270
Multianvil apparatus	1200	3000	94.8	1130

Note: SPS = spark plasma sintering.

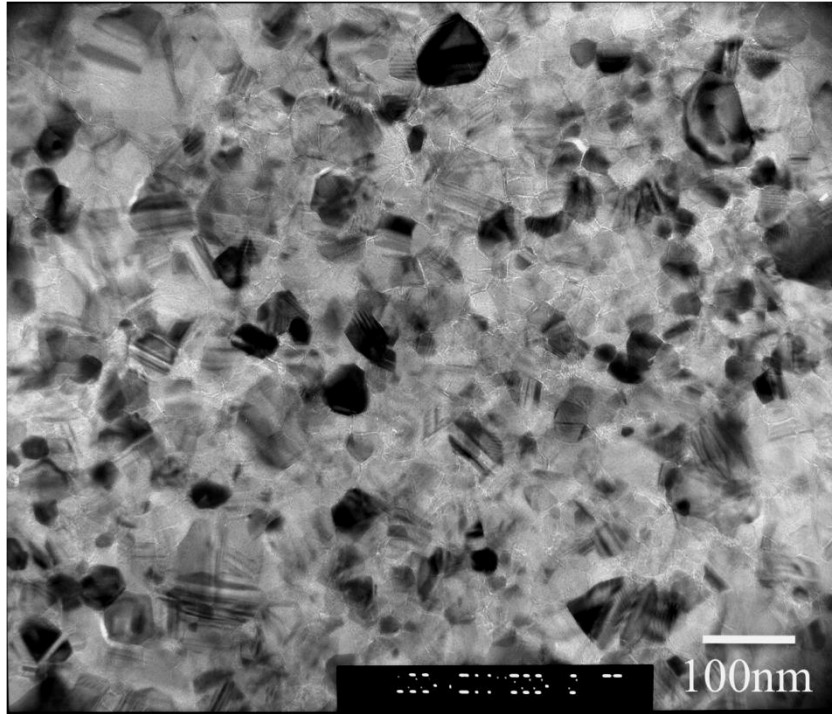


Figure 1. Ultra-high pressure HIP; 1600 °C, 980 MPa.

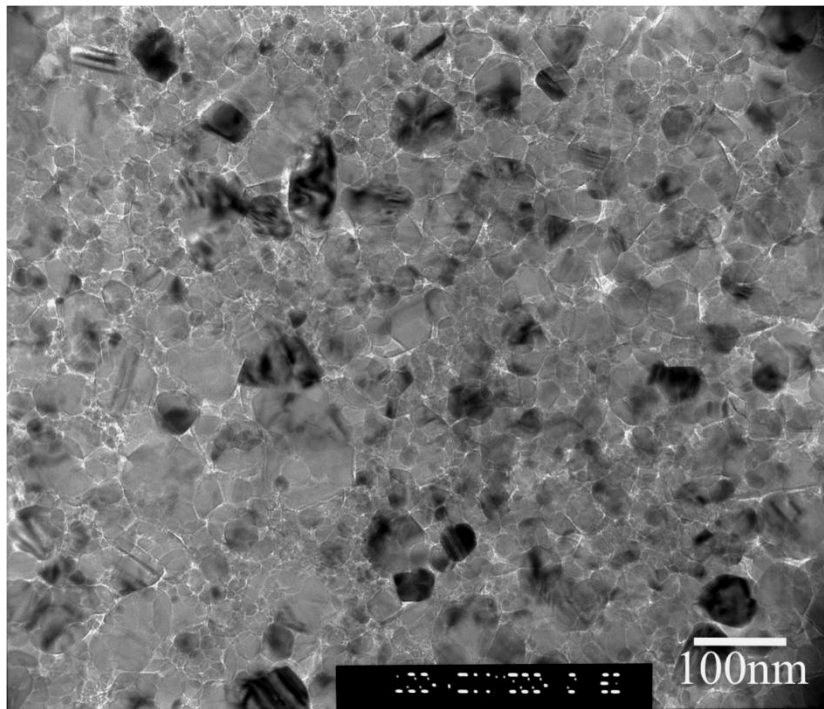


Figure 2. Multianvil high-pressure apparatus; 1200 °C, 3 GPa.

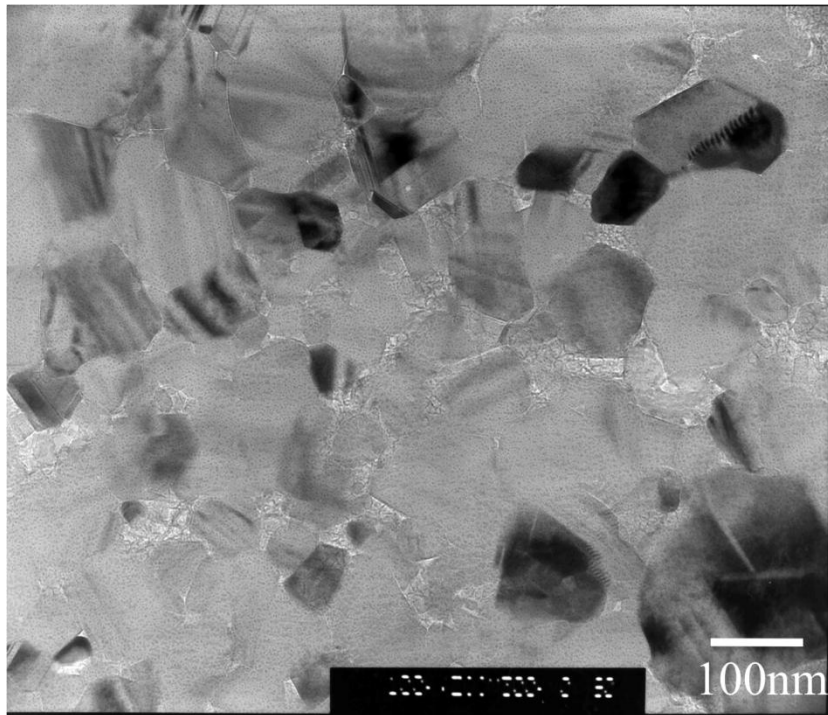


Figure 3. Standard HIP; 2000 °C, 200 MPa.

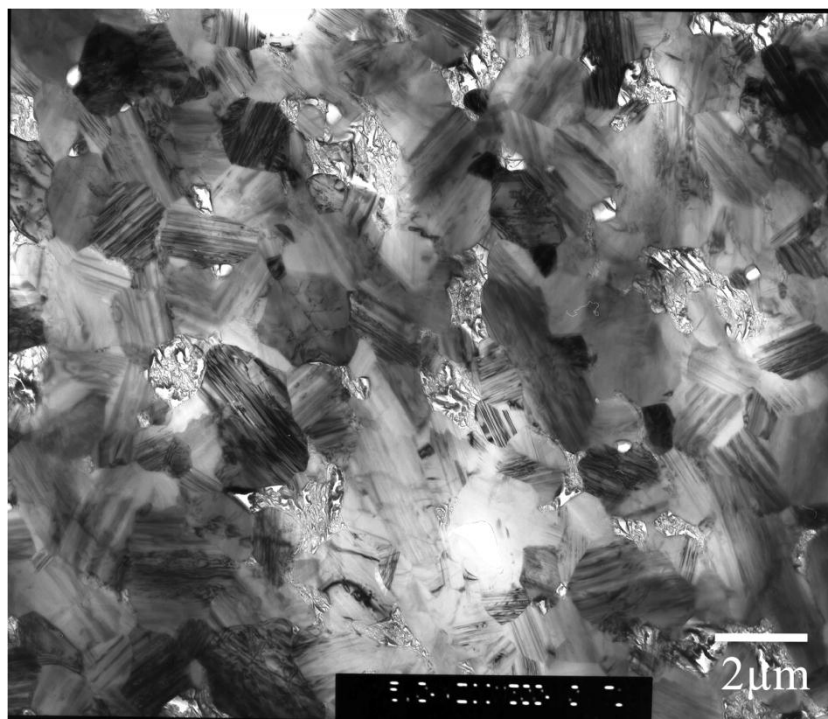


Figure 4. Sinter forging by SPS; 1800 °C, 500 MPa.

2.2 The Effect of the Grain Size on the Deformation at Elevated Temperature

The no-additive SiC ceramics with different grain sizes of 130 and 370 nm were prepared by annealing after HIPing. The strain rate $\dot{\epsilon}_0$ at elevated temperature is expressed as a function of the applied stress σ and grain size d as

$$\dot{\epsilon}_0 = A \frac{\sigma^n}{d^p} \exp\left(-\frac{Q}{kT}\right), \quad (1)$$

where n is the stress exponent, p is the grain size exponent, Q is the apparent activation energy for deformation, k is Boltzmann's constant, T is the temperature, and A is a constant. The stress exponent value was 2~3 and increased with decreasing strain rate. Such transition of stress exponent has been reported in superplastic zirconia ceramics and explained by the threshold model and/or the interface-controlled diffusion creep model. The origin of the transition of flow stress in SiC is currently unclear.

The flow stresses of SiC with smaller grain sizes were lower than those with larger grain sizes at a strain rate region of $>1 \times 10^{-5} \text{ s}^{-1}$ (figure 5). On the other hand, at a strain rate region of $<1 \times 10^{-5} \text{ s}^{-1}$, the flow stresses of SiC with smaller grain sizes were higher than those with larger grain sizes. Generally, the flow stress increases with increasing grain size in the superplastic deformation region. In this region, the deformation rate is controlled by diffusion. A novel interpretation is required for the inverse grain-size dependence at a lower strain rate. It is possible that dislocation gliding is a possible mechanism of this deformation behavior of SiC.

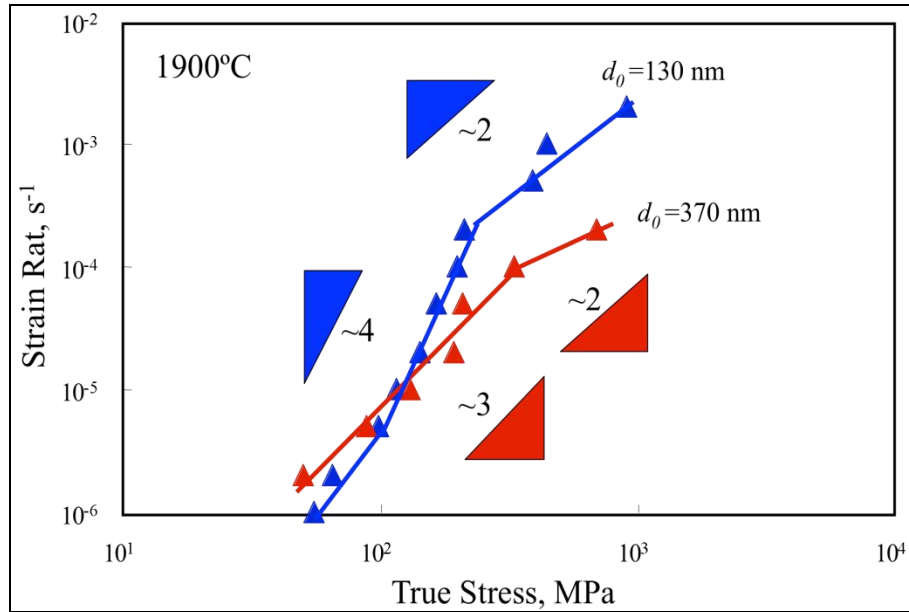


Figure 5. Relationship between stress and strain rate of SiC with different grain sizes.

2.3 Participation and Morphology of Dislocation Activity in Deformation of Nano-SiC Ceramics

Figure 6 indicates the relationship between grain size and calculated shear stress required for nucleation of dislocation in SiC. Because the shear modulus of SiC is very high, the critical shear stress is extremely high. This figure shows that a perfect dislocation was more easily nucleated than the partial dislocation in SiC with a larger grain size. On the other hand, the partial dislocation was more easily nucleated than a perfect dislocation in SiC with a smaller grain size. The critical grain size is ~400 nm. In both types of dislocations, the critical shear stress decreased with increasing grain size. The inverse grain-size dependence at the low stress region in figure 6 may relate to the dislocation activity as nucleation or gliding. Of course, the dominant mechanism of the nano-SiC is grain-boundary sliding. Moreover, the stress level to nucleate the dislocation was much higher than in the present experimental data. Therefore, dislocation gliding itself did not contribute to the total strain. It worked by accommodating stress concentration generated by the grain boundary sliding. If the grain size of nano-SiC were 130 nm, then the partial dislocation would be active.

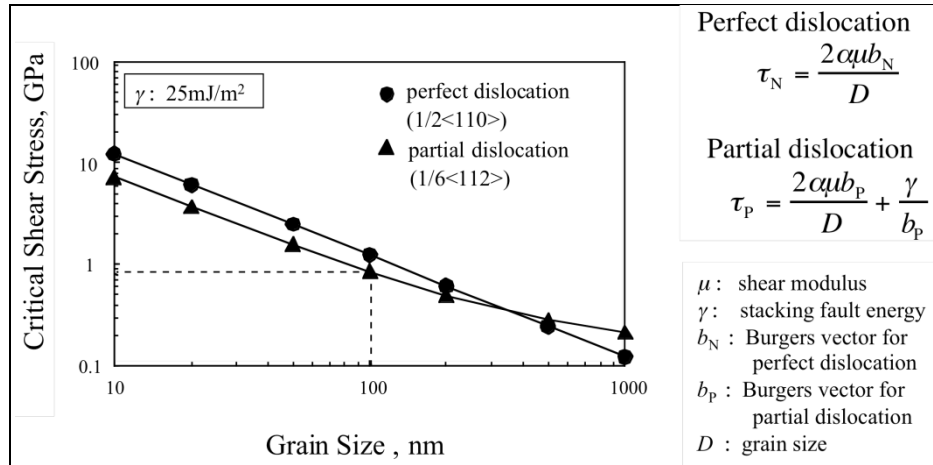


Figure 6. Relationship between grain size and shear stress required for nucleation of dislocation.

Figures 7–9 show transmission electron microscopy (TEM) micrographs of nano-SiC before and after deformation. After large deformation, the boundaries of the individual grains were not well defined and looked blurred, as in figure 2. The strain was stored in the grains. After annealing at 2100 °C, the stored strain seemed to disappear. The dislocations were hard to observe in SiC with the small grains. However, in SiC with the larger grains, they were often observed. We suspected that the movement of partial dislocations was important in the nano-SiC. Because the stacking fault energy of SiC was very low, it was reasonable for us to think that the partial dislocations moved through the nanograin, leaving the stacking faults.



Figure 7. TEM image before deformation.

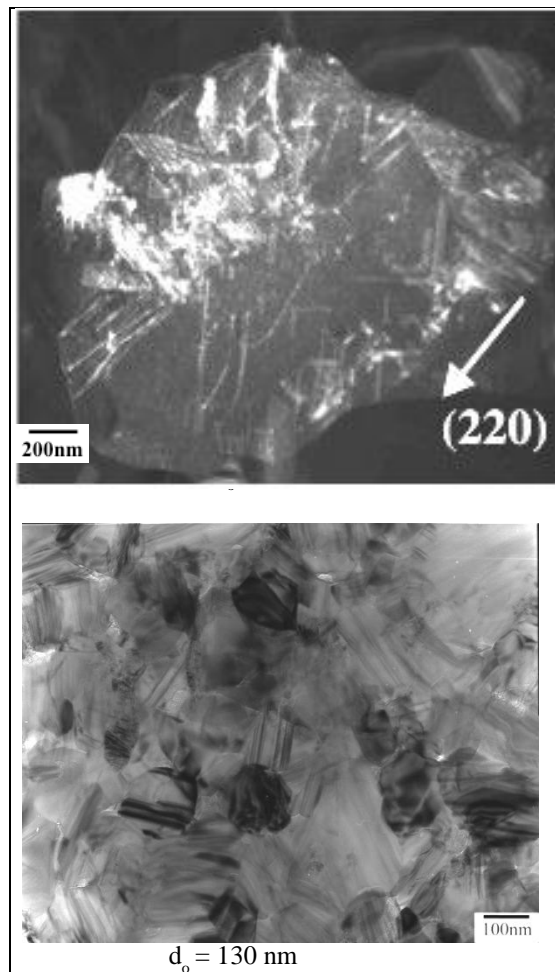


Figure 8. TEM image of deformed SiC
(1900 °C, $1 \times 10^4 \text{ s}^{-1}$, $\epsilon = 0.65$).

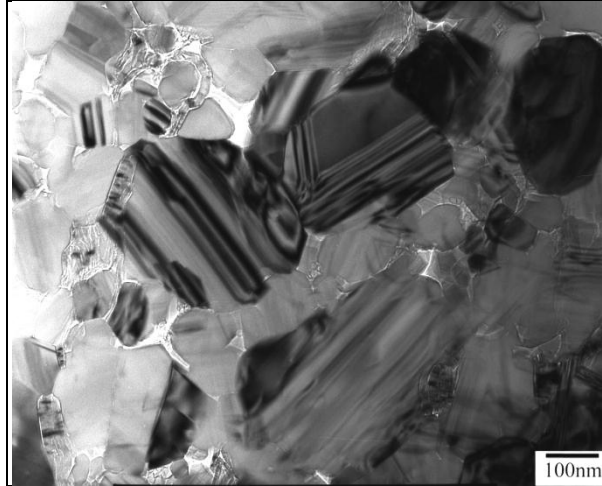


Figure 9. TEM image of annealed SiC (2100 °C, 1 h) after deformation.

2.4 The Effect of Carbon Content on the Deformation at Elevated Temperature

Nanosilicon powder was added to the β -SiC powder in order to control the carbon content. The mixed powder was sintered by hot-pressing to remove the impurity oxygen. The sintering was conducted at 2000 °C and 200 MPa using a SiC mold and SiC punches. The free carbon in SiC reacted with the impurity oxygen and added silicon as follows:

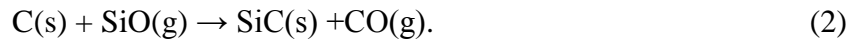


Figure 10 shows SEM micrographs of hot-pressed SiC. The grain size of SiC decreased with increasing the carbon and silicon content. This suggested that the excess carbon and silicon segregated at the grain boundary, decreasing the grain-boundary diffusivity. Such an effect was contrary to boron and oxygen. Table 2 shows the characteristics of hot-pressed SiC. Figure 11 illustrates the relationship between the amount of excess silicon and carbon and grain size.

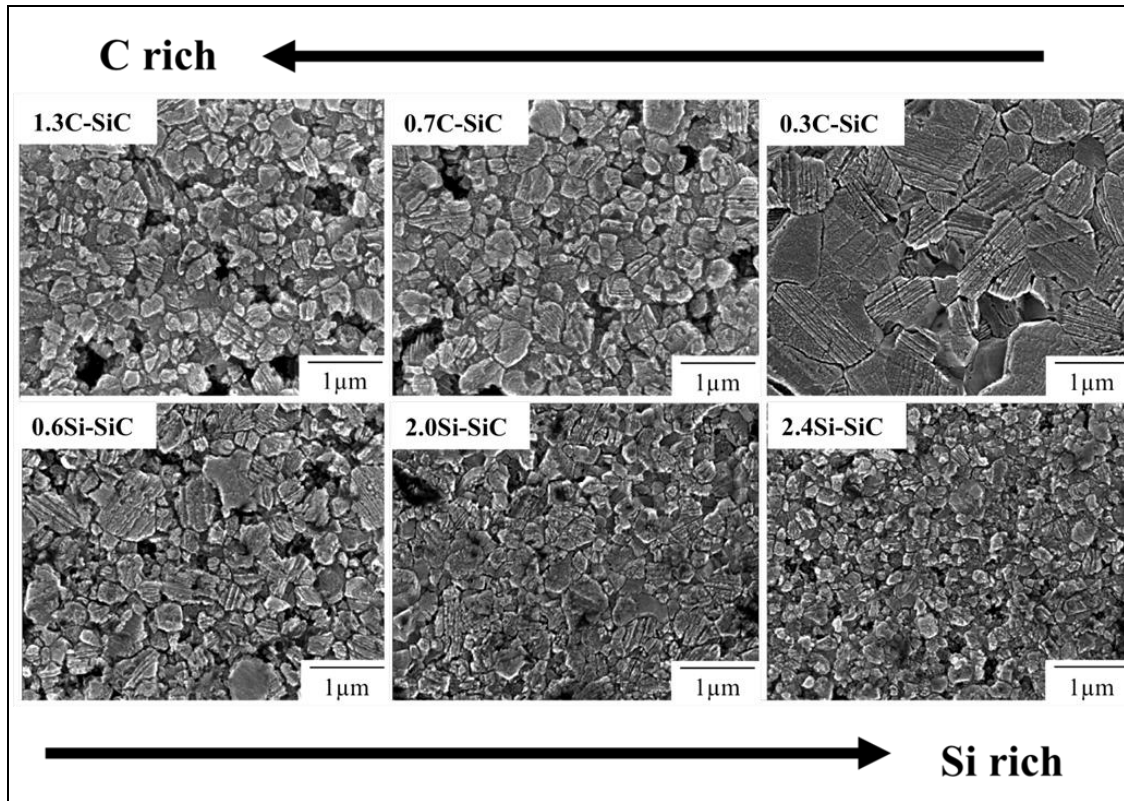


Figure 10. SEM micrographs of hot-pressed SiC.

Table 2. Hot-pressed SiC characteristics.

Designation	Excess Element (mol%)	Grain Size (nm)	Relative Density (%)
1.3C-SiC	1.3 (carbon)	350	95.5
0.7C-SiC	0.7 (carbon)	400	95.2
0.3C-SiC	0.3 (carbon)	760	98.9
0.6Si-SiC	0.6 (silicon)	470	97.4
2.0Si-SiC	2.0 (silicon)	400	98.1
2.4Si-SiC	2.4 (silicon)	270	97.9

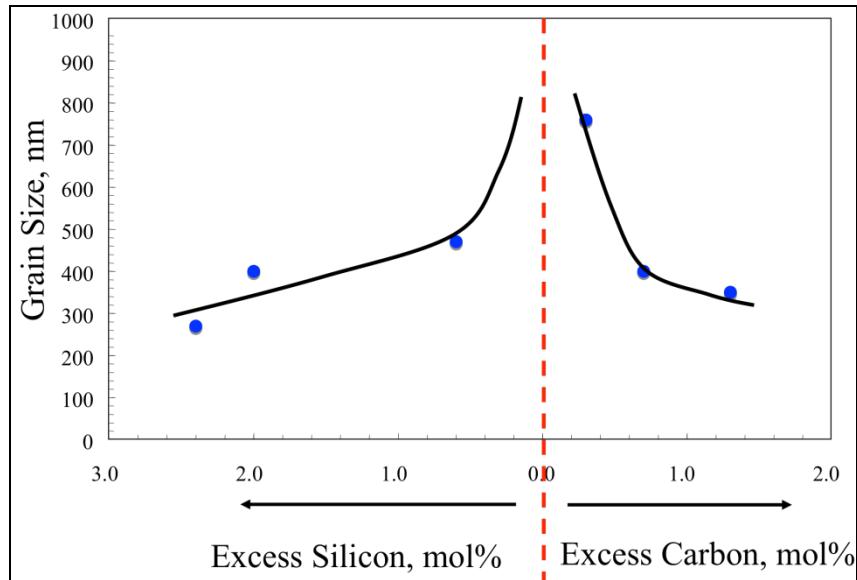


Figure 11. Relationship between the amount of excess carbon and silicon and grain size.

Figure 12 shows the relationship between the stress and strain rate in SiC with a different carbon and silicon content. The stress increased with increasing carbon content in spite of the decrease in grain size. The role of the excess carbon in SiC was quite the opposite of that of boron additive. The stress exponent tended to increase at a higher stress region. In this study, the effects of the excess carbon in pure SiC ceramics on the microstructure and deformation were revealed. The change of the structure and composition at the grain boundary by segregation of carbon atoms was interesting and will be researched in the future.

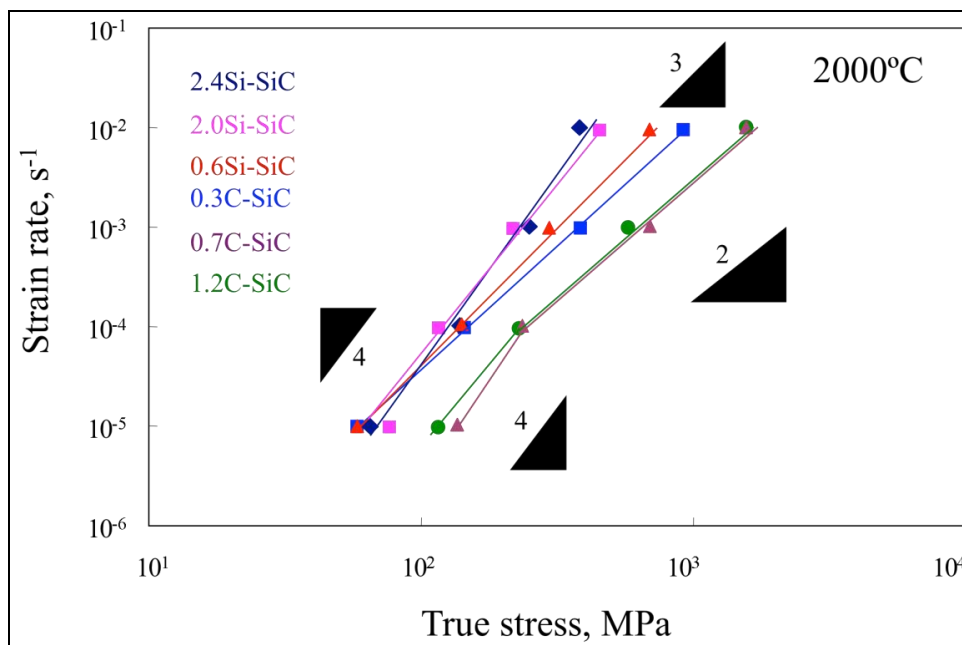


Figure 12. Relationship between stress and strain rate.

NO. OF
COPIES ORGANIZATION

1 DEFENSE TECHNICAL
(PDF INFORMATION CTR
only) DTIC OCA
8725 JOHN J KINGMAN RD
STE 0944
FORT BELVOIR VA 22060-6218

1 DIRECTOR
US ARMY RESEARCH LAB
IMAL HRA
2800 POWDER MILL RD
ADELPHI MD 20783-1197

1 DIRECTOR
US ARMY RESEARCH LAB
RDRL CIO LL
2800 POWDER MILL RD
ADELPHI MD 20783-1197

NO. OF
COPIES ORGANIZATION

1 PEO GCS
SFAE GCS BCT/MS 325
M RYZYI
6501 ELEVEN MILE RD
WARREN MI 48397-5000

1 ABRAMS TESTING
SFAE GCSS W AB QT
J MORAN
6501 ELEVEN MILE RD
WARREN MI 48397-5000

1 COMMANDER
WATERVLIET ARSENAL
SMCWV QAE Q
B VANINA
BLDG 44
WATERVLIET NY 12189-4050

1 COMMANDER
US ARMY AMCOM
AVIATION APPLIED TECH DIR
J SCHUCK
FT EUSTIS VA 23604-5577

1 USA SBCCOM PM SOLDIER SPT
AMSSB PM RSS A
J CONNORS
KANSAS ST
NATICK MA 01760-5057

1 UNIV OF DELAWARE
DEPT OF MECH ENGR
J GILLESPIE
NEWARK DE 19716

3 AIR FORCE ARMAMENT LAB
AFATL DLJW
D BELK
J FOSTER
W COOK
EGLIN AFB FL 32542

1 TACOM ARDEC
AMSRD AAR AEE W
E BAKER
BLDG 3022
PICATINNY ARSENAL NJ
07806-5000

NO. OF
COPIES ORGANIZATION

11 US ARMY TARDEC
AMSTRA TR R MS 263
K BISHNOI
D TEMPLETON (10 CPS)
WARREN MI 48397-5000

1 COMMANDER
US ARMY RSRCH OFC
A RAJENDRAN
PO BOX 12211
RSRCH TRIANGLE PARK NC
27709-2211

2 CALTECH
G RAVICHANDRAN
T AHRENS MS 252 21
1201 E CALIFORNIA BLVD
PASADENA CA 91125

5 SOUTHWEST RSRCH INST
C ANDERSON
K DANNEMANN
T HOLMQUIST
G JOHNSON
J WALKER
PO DRAWER 28510
SAN ANTONIO TX 78284

3 SRI INTERNATIONAL
D CURRAN
D SHOCKEY
R KLOOP
333 RAVENSWOOD AVE
MENLO PARK CA 94025 21

1 APPLIED RSRCH ASSOCIATES
D GRADY
4300 SAN MATEO BLVD NE
STE A220
ALBUQUERQUE NM 87110

1 INTERNATIONAL RSRCH
ASSOCIATES INC
D ORPHAL CAGE 06EXO
5274 BLACKBIRD DR
PLEASANTON CA 94566

1 BOB SKAGGS CONSULTANT
S R SKAGGS
7 CAMINO DE LOS GARDUNOS
SANTA FE NM 87506

NO. OF
COPIES ORGANIZATION

2 WASHINGTON ST UNIV
INST OF SHOCK PHYSICS
Y GUPTA
J ASAY
PULLMAN WA 99164-2814

1 COORS CERAMIC CO
T RILEY
600 NINTH ST
GOLDEN CO 80401

1 UNIV OF DAYTON
RSRCH INST
N BRAR
300 COLLEGE PARK
MS SPC 1911
DAYTON OH 45469-0168

1 COMMANDER
US ARMY TACOM
AMSTA TR S
L PROKURAT FRANKS
WARREN MI 48397-5000

1 PM HBCT
SFAE GCS HBCT S
J ROWE MS 506
6501 11 MILE RD
WARREN MI 48397-5000

3 COMMANDER
US ARMY RSRCH OFC
B LAMATINA
D STEPP
W MULLINS
PO BOX 12211
RSRCH TRIANGLE PARK NC
27709-2211

1 NAVAL SURFACE WARFARE CTR
CARDEROCK DIVISION
R PETERSON
CODE 28
9500 MACARTHUR BLVD
WEST BETHESDA MD 20817-5700

2 LAWRENCE LIVERMORE NATL LAB
R LANDINGHAM L369
J E REAUGH L282
PO BOX 808
LIVERMORE CA 94550

NO. OF
COPIES ORGANIZATION

3 SANDIA NATL LAB
J ASAY MS 0548
L CHHABILDAS MS 0821
D CRAWFORD ORG 0821
PO BOX 5800
ALBUQUERQUE NM 87185-0820

1 RUTGERS
THE STATE UNIV OF NEW JERSEY
DEPT OF CRMCS & MATLS ENGRNG
R HABER
607 TAYLOR RD
PICATINNY NJ 08854

1 THE UNIVERSITY OF TEXAS
AT AUSTIN
S BLESS
IAT
3925 W BRAKER LN STE 400
AUSTIN TX 78759-5316

1 CERCOM
R PALICKA
1960 WATSON WAY
VISTA CA 92083

6 GDLS
W BURKE MZ436 21 24
G CAMPBELL MZ436 30 44
D DEBUSSCHER MZ436 20 29
J ERIDON MZ436 21 24
W HERMAN MZ435 01 24
S PENTESCU MZ436 21 24
38500 MOUND RD
STERLING HTS MI 48310-3200

1 JET PROPULSION LAB
IMPACT PHYSICS GROUP
M ADAMS
4800 OAK GROVE DR
PASADENA CA 91109-8099

3 OGARA HESS & EISENHARDT
G ALLEN
D MALONE
T RUSSELL
9113 LE SAINT DR
FAIRFIELD OH 45014

NO. OF
COPIES ORGANIZATION

NO. OF
COPIES ORGANIZATION

1 CERADYNE INC
M NORMANDIA
3169 REDHILL AVE
COSTA MESA CA 96626

2 JOHNS HOPKINS UNIV
DEPT OF MECH ENGRNG
K T RAMESH
T W WRIGHT
3400 CHARLES ST
BALTIMORE MD 21218

2 SIMULA INC
V HORVATICH
V KELSEY
10016 51ST ST
PHOENIX AZ 85044

3 UNITED DEFENSE LP
K STRITTMATTER
E BRADY
R JENKINS
PO BOX 15512
YORK PA 17405-1512

10 NATL INST OF STANDARDS & TECH
CRMCS DIV
G QUINN
STOP 852
GAITHERSBURG MD 20899

2 DIR USARL
RDRL D
C CHABALOWSKI
V WEISS
2800 POWDER MILL RD
ADELPHI MD 20783-1197 23

ABERDEEN PROVING GROUND

60 DIR USARL
RDRL SL
R COATES
RDRL WM
S KARNA
P BAKER
J MCCAULEY (10 CPS)
RDRL WML
J NEWILL
M ZOLTOSKI
RDRL WML B
D TAYLOR (10 CPS)
RDRL WMM
R DOWDING

RDRL WMM A
J SANDS
T WEERASOORIYA
RDRL WMM D
E CHIN
K CHO
G GAZONAS
R SQUILLACIOTI
RDRL WMM E
J LASALVIA
P PATEL
RDRL WMM F
J MONTGOMERY
RDRL WMP
B BURNS
S SCHOENFELD
RDRL WMP B
C HOPPEL
M SCHEIDLER
RDRL WMP C
T BJERKE
J CLAYTON
D DANDEKAR
M GREENFIELD
S SEGLETES
W WALTERS
RDRL WMP D
T HAVEL
M KEELE
D KLEPONIS
H MEYER
J RUNYEON
RDRL WMP E
P BARTKOWSKI
M BURKINS
W GOOCH
D HACKBARTH
E HORWATH
T JONES
RDRL WML H
T FARRAND
L MAGNESS
D SCHEFFLER
R SUMMERS

INTENTIONALLY LEFT BLANK.